Astron. Astrophys. 338, L63–L66 (1998)

ASTRONOMY AND ASTROPHYSICS

LETTER

Letter to the Editor

CO study of the GM Aurigae Keplerian disk

A. Dutrey[1], **S. Guilloteau**[1], **L. Prato**[2], **M. Simon**[2], **G. Duvert**[3], **K. Schuster**[1], **and F. Ménard**[3]

[1] Institut de Radio Astronomie Millimétrique, 300 Rue de la Piscine, F-38406 Saint Martin d'Hères, France
[2] Department of Physics and Astronomy, State University of New York, Stony Brook, NY 11794-3800, USA
[3] Laboratoire d'Astrophysique de Grenoble, B.P. 53, F-38041 Grenoble Cedex 9, France

Received 15 June 1998 / Accepted 25 August 1998

Abstract. We report new high resolution ($0.6 - 1.7''$) images of GM Aur in the ^{12}CO J $= 2 \rightarrow 1$ line and the 1.3 and 2.7 mm continuum. The dust disk, located at the center of the CO disk, is resolved by the $0.6''$ beam of the interferometer. We derive a minimum radius of ~ 200 AU, and a total mass (dust+gas) of about $\sim 0.025\,\mathrm{M}_\odot$. Our CO observations also resolve the Keplerian rotation of the gas disk. Since the CO emission is optically thick, the CO data does not allow a disk mass measurement but we can estimate the dynamical mass of the system, i.e. the *stellar mass*, $M_* = 0.84 \pm 0.05 \times (D/140\,\mathrm{pc})\,\mathrm{M}_\odot$ although a solution with a more inclined disk and lower stellar mass ($\sim 0.6\,\mathrm{M}_\odot$) is also possible.

Key words: stars: T Tauri – circumstellar matter – pre-main sequence – radio-lines: stars

1. Introduction

Observations of young stars in the sub-mm and mm-wavelength continuum provide strong evidence for the theoretical expectation that they are surrounded by evolving, circumstellar disks (e.g. Beckwith et al. 1990, B90). However, only angularly resolved kinematic data can discriminate among, for example, rotating disks, infalling material, and outflows. Since young stars are usually in or near molecular cloud material with various velocity components, it has proven difficult to obtain data whose interpretation is unambiguous.

GM Aur is a single, classic T Tauri (cTT) star located at ~ 140 pc distance at the edge of the CO emission associated with L 1517 (Herbig & Bell 1988; Elias 1978). With an estimated age of 2×10^6 to $\sim 10^7$y, GM Aur is relatively old compared to other stars in Taurus-Auriga (B90, Simon & Prato 1995). Koerner et al. (1993, K93) detected the molecular emission of the cold outer circumstellar disk by interferometry of the ^{13}CO J $= 2 \rightarrow 1$ line. These and subsequent interferometric observations at ~ 2" resolution, and *Hubble Space Telescope* images show a flared disk in rotation at inclination $\sim 60^\circ$ and position angle $\sim 60^\circ$ (Koerner 1997, Stapelfeldt et al. 1995). The upgrade of the IRAM interferometer to dual-frequency receivers (2.7 and 1.3 mm) and an extension of the baselines now provides resolution below 1–1.5″. We therefore began a new series of observations to improve our understanding of the circumstellar material around GM Aur.

Send offprint requests to: A.Dutrey

2. Observations

Our IRAM interferometer observations used 4 antennas operating in snapshot mode (Guilloteau et al. 1992, Dutrey et al. 1996, D96). We observed simultaneously at 110.2 GHz and 230.5 GHz (^{12}CO J $= 2 \rightarrow 1$) in the lower side-band. The back end was a correlator with one band of 20 MHz centered on the ^{12}CO J $= 2 \rightarrow 1$ line, 3 bands of 160 MHz for the 1.3 mm continuum, and 2 bands of 160 MHz for the 2.7 mm continuum. The spectral resolution was 0.18 $\mathrm{km\cdot s^{-1}}$ in the narrow band. The phase and flux calibrators were 0415+379 and 0528+134. The rms phase noise was 8° to 25° and 15° to 50° at 2.7 mm and 1.3 mm, respectively, which introduced position errors of $< 0.1''$. During our observations, the flux of 0415+379 increased from 5.5 to 10.5 Jy and 3.5 to 9.5 Jy at 2.7 mm and 1.3 mm, respectively. We used the calibrators to estimate the seeing, which was below $\sim 0.3''$. Baselines up to 400 m provided $\sim 0.7''$ resolution for the 1.3 mm continuum data and 1.4″ at 2.7 mm; because of limited sensitivity, the ^{12}CO J $= 2 \rightarrow 1$ data was tapered to 1.7″. The total on source integration time is only 4 hours. We used the GILDAS software package to reduce the data. The continuum images are the results of summing the lower and the upper side-band data. We used natural weighting of the visibilities for both the continuum and line maps. We did not subtract the continuum emission from the CO map.

3. Results

Table 1 lists the results of our continuum measurements. The 1.3 and 2.7 mm fluxes agree very well with K93's and D96a's values. The difference with B90 seems acceptable considering the broad bandwidth of their bolometer measurement. The continuum source is clearly resolved at 1.3 mm (Fig. 1). We determined the size and orientation of the continuum emission by

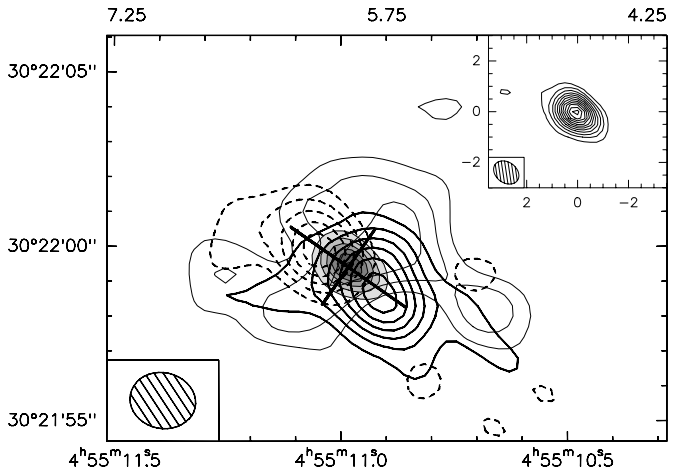

Fig. 1. Contours of ^{12}CO J $= 2 \rightarrow 1$ emission at 4.5, 5.75 (systemic), and 7.0 km/s (synthesized beam $1.9'' \times 1.6''$ at PA 86°), superposed on the continuum image at 1.3 mm in grey scale. The CO contour steps are 250 mJy/beam. The continuum image (synthesized beam $0.6'' \times 0.7''$ at PA 56°) is shown in the insert; the contour steps are 7.5 mJy/beam. The cross indicates the position, orientation and aspect ratio of the 1.3 mm continuum peak. Both the CO and continuum emission peak at $RA = 4^h55^m10.98^s$ and DEC $= 30^o21'59.5''$ (J2000.0).

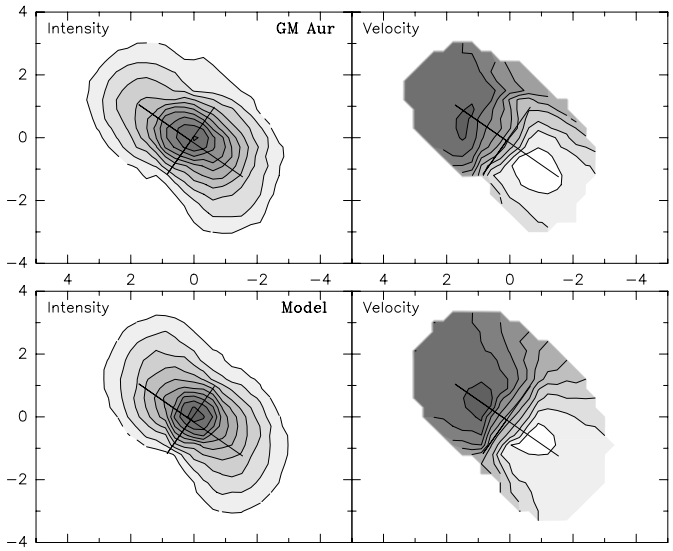

Fig. 2. Top row: CO J=2-1 total intensity map (left) and velocity gradient (right). Bottom row: same as above from the best model. The cross in each panel is the same as in Fig. 1. A threshold of 0.5 Jy/beam was used in computing the intensity and velocity images from the channel maps.

fitting elliptical Gaussians to the visibilities (Table 1). The position angle determined from the spectroscopic line measurement is mainly affected by the precision of the RF bandpass and delay tracking. The continuum data are sensitive to the accuracy of the amplitude calibrations, and therefore provide an independent determination of the position angle. Our measured values agree very well with each other.

Table 1. Continuum measurements

λ (mm)	Flux Density mJy	Diameter $''\times''$	Ref.
0.77	850±90	≤ 20	BS91
1.3	253±12	≤ 10	B90
1.4	181±27	≤ 5	K93
2.7	27.7±2.2	1.24±0.25	D96
1.3	169.7 ± 3.7	$1.07 \pm.05 \times .63 \pm.05$ P.A.$\simeq 57 \pm 5^\circ$	this
2.7	27.7 ± 2.1	$1.25 \pm.20 \times .65 \pm.17$ P.A.$\simeq 58 \pm 11^\circ$	paper

Fig. 1 shows the superposition of the continuum emission at 1.3 mm (grey scale) and ^{12}CO J $= 2 \rightarrow 1$ line emission at the systemic, redshifted, and blueshifted velocities (thin, dashed and thick contours, respectively). Fig. 2 and 3 compare results derived from the observations and our models. The top left panel of Fig. 2 shows that the centroids of the spatial distribution of the velocity integrated CO line emission and the 1.3 mm continuum emission coincide to high accuracy. The velocity gradient of the CO emission (Fig. 2, top right) lies along the continuum major axis, which indicates that the emission arises in a disk rotating about an axis at a position angle of $141^\circ \pm 2^\circ$ (as deduced from the χ^2 fit performed on the CO data). Fig. 3 shows the individual velocity channel maps from which Fig. 1 is derived. The peak values of the observed brightness temperature, for example ~ 8 K at the systemic velocity, are close to the ~ 10 K kinetic temperature expected in the outer regions of the disk (see below). This indicates that the line emission is optically thick.

If we assume that the apparent ellipticity of the CO emission represents the projection of a circular disk, then its inclination is $i_{co} \sim 54^\circ \pm 5$, with 0° meaning face-on. An elliptical Gaussian fit to the 1.3 mm continuum emission implies an inclination angle of $i_d \sim 54^\circ \pm 5$ (and $i_d \sim 58^\circ \pm 14$ from the 3 mm data). Values i_d derived from the continuum are lower limits because of seeing effects, while i_{co} is independent of the seeing because it is measured on much larger scales. However, correcting for the estimated seeing ($0.3''$) only increases i_d to 57°. Our values for the disk inclination and PA are in agreement with the values reported by Koerner (1997) and Stapelfeldt et al. (1995).

4. Disk Properties

To determine the disk properties, we used a standard model of Keplerian disk in hydrostatic equilibrium (see D94, and Table 2 for the parameter names) and performed a χ^2 minimization on the main parameters as described in Guilloteau and Dutrey 1998 (GD98). The minimization was directly made inside the visibilities. The disk orientation and systemic velocity were solved for together (giving PA$= 51^\circ$ and $V_{LSR} = 5.62\,\mathrm{km{\cdot}s^{-1}}$), and a global fit was made for the 5 most important parameters of the model (T_{100},V_{100},i,R_{out} and q). This ensures a proper determination of the dynamical mass (see GD98). Parameters for the

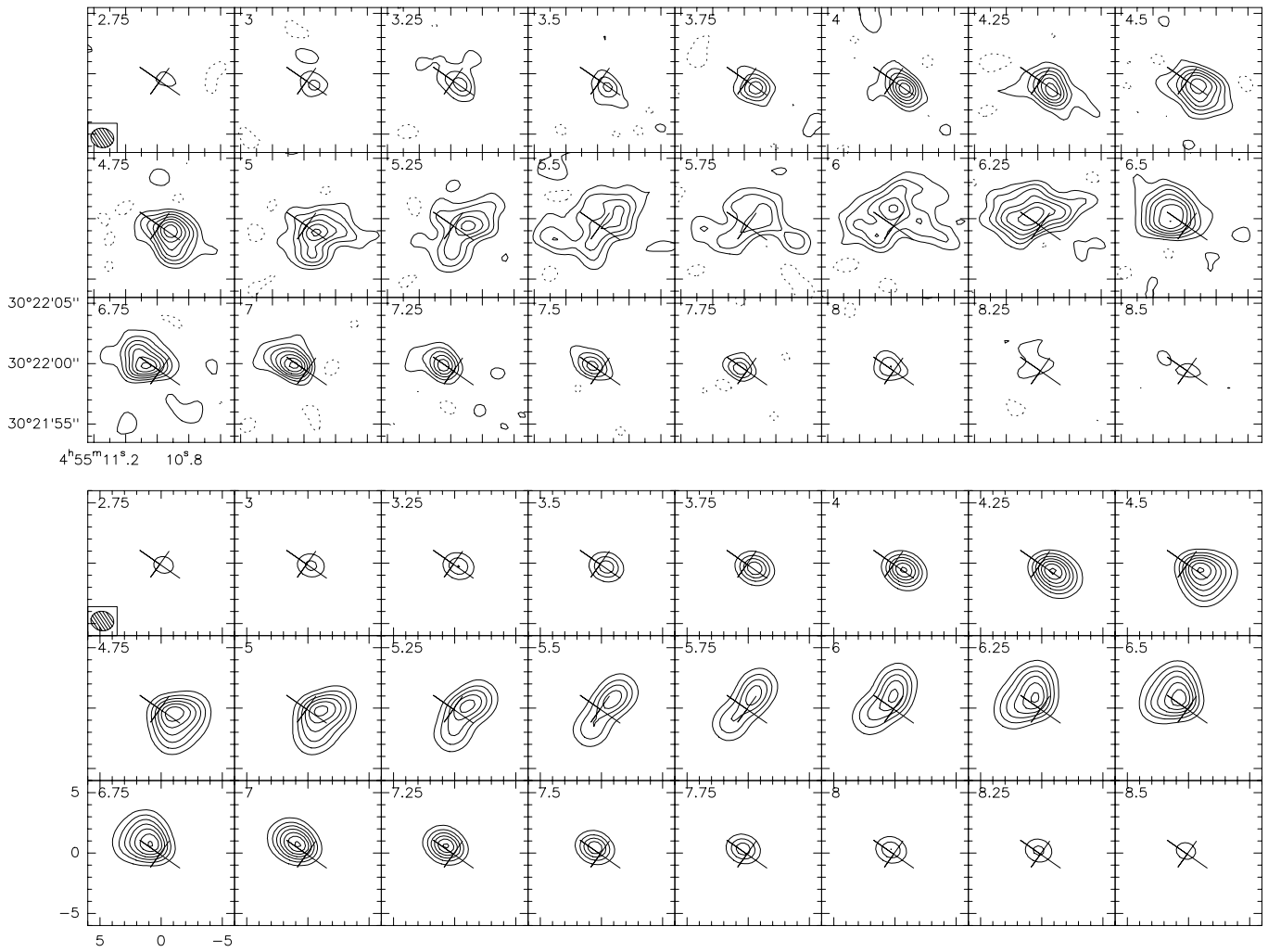

Fig. 3. Channel maps of the CO data (top) and the best model processed in identical way (bottom). Contour steps are 0.25 mJy/beam (or 1.9 K). Velocities are indicated in the upper left corner of each panel.

best model are summarized in Table 2 and the results are compared with the observations in the lower half of Fig. 2 and Fig. 3. We also found that a moderate turbulent velocity is required to best model the CO data.

The disk inclination determines the central mass M_* because the radial velocity is proportional to $\sqrt{M_*} \times sin(i)$. Therefore high angular resolution data can provide accurate measurement of M_* if the inclination is properly measured. From our χ^2 minimization, we find two possible solutions for i: $56 \pm 2°$ or $70 \pm 6°$. They correspond respectively to dynamical masses $M_* = (0.84 \pm 0.05) \times (D/140\,\mathrm{pc})\,\mathrm{M}_\odot$ and $M_* = (0.62 \pm 0.08) \times (D/140\,\mathrm{pc})\,\mathrm{M}_\odot$ (errors are given at 2σ and include uncertainties on i). Since the disk mass is very small, the dynamical mass is essentially the stellar mass. We favor the first solution given the inclination $i_d \sim 57°$ determined from the dust emission.

However, we cannot definitely reject the second (low mass) solution. Fig. 2 suggests that the CO emission may be slightly twisted compared to the mean PA, with the inner disk at higher PA. This variation may indicate that the disk is warped, or that the velocity pattern is not fully Keplerian (for the velocity law: we found $v = 0.5 \pm 0.1$, see Table 2). Some confusion with the surrounding molecular cloud may also contaminate the CO rotation pattern. Complementary observations with higher sensitivity and angular resolution, or in another molecular tracer, would be required to disentangle these possibilities. The kinematic method to determine stellar mass is nonetheless very promising because it is independent of stellar properties and evolutionary tracks.

The observations show that the ^{12}CO J $= 2 \rightarrow 1$ line emission is optically thick. The line emission is therefore a good tracer of the gas kinetic temperature, T_k, at the surface $\tau_{CO(2-1)} \sim 1$ of the disk. However, because the opacity is extremely high, the kinetic temperature deduced from the CO observations may not be representative of the inner parts or the cooler parts of the disk, where most of the mm-wave continuum emission of the optically thin dust originates. We can also use the fact that we do not see through the disk in the ^{12}CO J $= 2 \rightarrow 1$ line in order to deduce its three dimensional structure. Fig. 3 shows that the CO line emission at velocities near

Table 2. Parameter description for the GM Aur disk

Distance	D (pc)	140	
Systemic velocity	V_{LSR} (km.s^{-1})	$5.62\pm$	0.03
Orientation	PA	$51\pm$	2°
Inclination	i	$56\pm$	2°
^{12}CO abundance	X(^{12}CO)	$1.4 \cdot 10^{-5}$	
Outer radius	R_{out} (AU)	$525\pm$	20
Turbulent linewidth	Δv (km.s^{-1})	$0.17\pm$	0.04
Density law: $n(r) = n_{100}(\frac{r}{100\mathrm{AU}})^{-s}$			
density at 100 AU	n_{100} (cm^{-3})	$4\ 10^8$	
density exponent	s	2.75	
Temperature law: $T(r) = T_{100}(\frac{r}{100\mathrm{AU}})^{-q}$			
temperature at 100 AU	T_{100} (K)	$37\pm$	2
temperature exponent	q	$0.64\pm$	0.06
Velocity law: $V(r) = V_{100}(\frac{r}{100\mathrm{AU}})^{-v}$			
velocity at 100 AU	V_{100} (km.s^{-1})	$2.78\pm$	0.10
velocity exponent	v	$0.5\pm$	0.1
star mass	M$_*$ (M$_\odot$)	$0.84\pm$	0.05
Dust disk size	R_d (AU)	$>$	200
total mass	M_d (M$_\odot$)	~ 0.025	

The errors are the 2σ formal errors from the χ^2 fit.

the systemic velocity is brighter in the northern part of the disk than in the southern part. This north-south asymmetry can be explained as an effect of self-absorption in a slightly geometrically thick disk. In the southern part, the line-of-sight first enters a colder layer of material. Since the temperature decreases with increasing radius, the inclination indicates that the southern side is the nearest. This self-absorption effect is well reproduced by the model.

We found that the radial dependence of the kinetic temperature $q = 0.5$ used to model the GM Aur disk emission by B90 and K93 does not accurately reproduce the observed centrally peaked CO emission (down to $R \geq 80 - 100$AU from the central star) because it produces too strong emission in the outer parts of the disk; this solution is rejected at 4σ. We obtain the best fit with a steeper profile corresponding to $q = 0.64$, which gives $T_k(R_{out}) \sim 10$ K. Such a kinetic temperature law implies a scale height (as defined by Pringle 1981), $h_D \propto r^{1.20}$.

Since the CO line is optically thick, we cannot measure the total disk mass. Unlike CO, the dust emission is essentially optically thin, even at 1.3 mm, with a brightness temperature given by $\Sigma(r) \times T_k(r) \times \kappa_d \propto r^{-(p+q)}$ which falls below our sensitivity curve at large radius.

Following D96, from the 3 mm and 1.3 mm emission angular size of $\sim 1.1''$, we deduce a minimum outer radius for the dust disk of $\sim$ 200 AU, and that the power law index of the surface density distribution $\Sigma(r) \propto r^{-p}$ must not be too steep. The 3 mm and 1.3 mm continuum data are fully consistent with the model parameters presented in Table 2 which give $p = s + q/2 - 1 - v = 1.56$ and $R_{out} = 525$ AU. Hence, the dust and CO gas could originate in the same medium even if the apparent dust radius is significantly smaller than R_{out}. Nevertheless, these observations cannot exclude that the dust is confined to a significantly smaller region ($R_d \sim 200$ AU).

Because of very different opacities and detection bandwidths, *continuum and CO observations do not sample the same region of the disk*. We estimate that our continuum data are sensitive to material located from $\sim$ 10 up to $\sim$ 200 AU from the star while CO data only trace the gas down to a radius of $\sim 80 - 100$ AU. A direct comparison of both tracers is then not easily possible and becomes impossible in our case because the CO line is optically thick (see Sect. 3). With a dust absorption coefficient $\kappa(\nu) = 0.1(\nu/10^{12}\mathrm{Hz})^\beta$, we also find $\beta \simeq 1$, and a total mass of (gas+dust) 0.025 M$_\odot$ reproduce the observed continuum flux. This is on the same order as the protosolar nebula mass.

5. Summary

Our CO observations show a large Keplerian disk ($R_{out} \sim 525$ AU) around a star of $(0.84 \pm 0.05) \times (D/140\,\mathrm{pc})\,\mathrm{M}_\odot$, although a solution with a more inclined disk and lower stellar mass ($\sim 0.6\,\mathrm{M}_\odot$) is also possible. Self-absorption in the CO map indicates that the disk is flared (or at least has a small thickness), with the southern side pointing towards us. The kinetic temperature deduced from the CO data is steeper than previous estimates, most likely around $\propto r^{-0.64}$, implying a scale height $\propto r^{1.2}$. The dust disk, located at the center of the CO disk, contains about ~ 0.025 M$_\odot$. It extends at least up to 200 AU, and could even be identical to the CO disk.

Since the GM Aur disk is fully resolved by the IRAM array, it is an excellent candidate for further study. In particular, high sensitivity mapping of optically thin lines of CO isotopomers will measure the mass of the outer disk and enable comparison of the gas and dust distribution.

Acknowledgements. We thank J. Bouvier and R. Mathieu for information about the visible light variability and radial velocity observations of GM Aur and L. Hartmann, G. Herbig, and K. Strom for information about its spectral type. LP and MS were supported in part by NASA Origins of Solar Systems Grant NAGW 4113 and NSF Grant 94-17191.

References

Beckwith, S.V.W., et al 1990, AJ, 99, 924
Beckwith, S.V.W & Sargent, A.I., 1991, ApJ 381, 250 (BS91)
Dutrey, A., Guilloteau, S. & Simon, M., 1994, A&A 286, 149 (D94)
Dutrey, A., et al, 1996, A&A 309, 493 (D96)
Elias, J.H., 1978, ApJ 224, 857
Guilloteau, S. et al, 1992, A&A 262, 624
Guilloteau, S. & Dutrey, A. 1994, A&A 291, L23
Guilloteau, S. & Dutrey, A. 1998, A&A accepted (GD98)
Herbig, G., & Bell, K.R. 1988, *Lick Obs. Bull.* No. 1111
Koerner, D.W., et al 1993, Icarus 106,2 (K93)
Koerner, D.W. 1997, Origins of Life and Evolution of the Biosphere, 27, 157
Pringle, J.E. 1981, AARA 19,137
Simon, M. & Prato, L. 1995, ApJ 450, 824
Stapelfeldt, K.R. etal, 1995, BAAS, 187, 113.04